Submicrometer aerosol particle size distribution and hygroscopic growth measured in the Amazon rain forest during the wet season

Jingchuan Zhou and Erik Swietlicki

Division of Nuclear Physics, Lund University, Lund, Sweden

Hans Christen Hansson

Institute of Applied Environmental Research, Stockholm University, Stockholm, Sweden

Paulo Artaxo

Department of Physics, University of São Paulo, São Paulo, Brazil

[1]   The number-size distribution and hygroscopic growth of submicrometer aerosol particles were measured in central Amazonia during the first Cooperative LBA Airborne Regional Experiment (CLAIRE) wet season experiment in March–April 1998. This was the first time ever that these types of measurements were performed in the Amazon rain forest. A Differential Mobility Particle Sizer (DMPS) was used to measure aerosol number-size distribution with diameters in the range 3–850 nm. The observed total number concentrations were frequently between 300 and 600 cm^{-3} with a mean value around 450 cm^{-3}. Two aerosol particle modes (Aitken and accumulation mode) were always present. The average particle concentrations for those two modes were 239 and 177 cm^{-3}, with geometric diameters of 68 and 151 nm, respectively. An ultrafine mode had a number concentration and a mean diameter of 92 cm^{-3} and 24 nm, respectively, and only occurred at 18% of the time, causing the size distribution to be trimodal instead of bimodal. The hygroscopic growth of aerosol particles was measured in situ with a Hygroscopic Tandem Differential Mobility Analyzer (H-TDMA) at six dry particle diameters between 35 and 265 nm. In contrast to the bimodal hygroscopic behavior found in polluted continental environments, the hygroscopic properties of aerosol particles in the Amazon rain forest is essentially unimodal with average diameter growth factors of 1.16–1.32 from dry to 90% relative humidity (RH). Aerosol soluble volume fractions were, in general, between 0.14 and 0.27, estimated by assuming that only ammonium hydrogen sulphate interacted with water vapour.   INDEX TERMS: 0305 Atmospheric Composition and Structure: Aerosols and particles (0345, 4801); 0322 Atmospheric Composition and Structure: Constituent sources and sinks; 0365 Atmospheric Composition and Structure: Troposphere—composition and chemistry; KEYWORDS: CLAIRE, TDMA, DMPS, Amazon rain forest, size distribution, hygroscopicity

Citation: Zhou, J., E. Swietlicki, H. C. Hansson, and P. Artaxo, Submicrometer aerosol particle size distribution and hygroscopic growth measured in the Amazon rain forest during the wet season, *J. Geophys. Res.*, *107*(D20), 8055, doi:10.1029/2000JD000203, 2002.

1.   Introduction

[2]   The Amazon Basin is the world's largest rain forest and as such a particularly important ecosystem. Over the Amazon rain forest, intense convective activity provides a rapid vertical mixing of biogenic gases and aerosol into the troposphere and has an impact on the global tropospheric chemistry [*Garstang et al.*, 1988], especially during the wet season [*Harriss et al.*, 1990]. In response to the worldwide concern about the fate of tropical rain forest and about the global implications of the changes which the Amazon region has been undergoing, the Large Scale Biosphere–Atmosphere Experiment in Amazonia (LBA) was planned

to take place in the Amazon over 1997–2003 (LBA Homepage, 1998, available at http://lba.cptec.inpe.br/lba/indexi.html). As part of the LBA, the first Cooperative LBA Airborne Regional Experiment (CLAIRE) field experiment took place during the wet season in March and April 1998 in the northern and central Amazon Basin. Coordinated ground and aircraft measurements were conducted to study biological emissions and atmospheric transformations of trace gases, sources, composition and properties of atmospheric aerosol (LBA-CLAIRE Homepage, 1998, available at http://www.mpch-mainz.mpg.de/~claire/CLAIRE.htm).

[3]   The Lund Aerosol Group participated in the CLAIRE experiment and contributed with measurements of aerosol particle number-size distributions and hygroscopic growth at a ground station near Manaus. The aerosol particle size distribution and its temporal and spatial

variability is a fundamental aerosol property. Of nearly equal importance is the aerosol hygroscopicity, which determine the ambient particle size at water vapour subsaturation, and the separation of particles at supersaturation between those that activate and form cloud droplets and those that remain as an interstitial aerosol. The optical properties of both the aerosol and the ensemble of cloud droplets are decided by the chemical composition and hygroscopic properties of the aerosol particles and cloud droplets. The number-size distributions and hygroscopic properties of the submicrometer aerosol particles are thus crucial properties for the life cycle of the Amazonian aerosol, as well as the radiative forcing of aerosols on Amazonia and global climate.

[4] The study of the Amazonian aerosols has received considerable attention in the last two decades. Those studies were mostly carried out within comprehensive international experiments, such as the Amazon Boundary Layer Experiment: dry season 1985 (ABLE 2A) [*Artaxo et al.*, 1988; *Browell et al.*, 1988; *Harriss et al.*, 1988; *Talbot et al.*, 1988; *Wouters et al.*, 1993], the Amazon Boundary Layer Experiment: wet season 1987 (ABLE 2B) [*Artaxo et al.*, 1990; *Browell et al.*, 1990; *Gregory et al.*, 1990; *Harriss et al.*, 1990; *Talbot et al.*, 1990; *Wouters et al.*, 1993] and the Smoke, Clouds, and Radiation-Brazil experiment 1990 (SCAR-B) [*Artaxo et al.*, 1998; *Echalar et al.*, 1998; *Eck et al.*, 1998; *Kaufman et al.*, 1998; *Kotchenruther and Hobbs*, 1998; *Remer et al.*, 1998]. From these experiments, three main types of aerosol sources were identified and analyzed: biomass burning, natural biogenic emissions, and soil dust resuspension. However, those aerosol studies mostly employed mass and bulk analytical techniques thus had difficulties in providing information on aerosol number-size distribution (especially for the ultrafine and Aitken mode aerosols).

[5] During the recent decade, the differential mobility analyzer (DMA) has developed into an especially powerful tool for the particle size analysis of submicrometer aerosols [*Flagan*, 1998]. DMA based aerosol number-size distribution and hygroscopicity measurements have been carried out in continental areas [e.g., *Zhang et al.*, 1993; *Svenningsson et al.*, 1997; *Swietlicki et al.*, 1999], as well as in various remote marine areas [e.g., *Covert et al.*, 1996a, b; *Bates et al.*, 1998; *Berg et al.*, 1998; *Swietlicki et al.*, 2000; *Zhou et al.*, 2002]. However, no such study involving submicrometer aerosols in the tropical forest has been performed prior to the one presented here.

2. Experimental
2.1. Field Site and Meteorological Conditions

[6] The measurements were performed during the LBA-CLAIRE 1998 (CLAIRE-98) experiment in March and April, at a ground station located 125 km northeast of Manaus at Balbina (1°56′S, 59°25′W), in Amazonia, Brazil.

[7] Local observations of radiation, temperature, relative humidity (RH), and wind speed all showed distinct diurnal variations (radiation: daytime maxima $300-900$ W · m^2; temperature: night-time minima $22-26°$C, daytime maxima $26-35°$C; RH: night-time minima $50-90\%$, daytime maxima $80-100\%$; wind speed rarely >3 m·s^{-1}). Figures showing the temporal variation of these parameters and ozone can

be found in the work of *Kesselmeier et al.* [2000]. Rainfall rates are shown in Figure 2a. The overall weather conditions during the campaign were characteristic of the Amazonian wet season.

[8] Local winds were from NE to SE during daytime, and E to SSE at night. Air mass backward trajectories at the 975 hPa level (on arrival at Balbina) came exclusively from NE-E, and crossed the Atlantic coast between French Guyana and the Amazon delta before entering over South America. Higher levels trajectories (850 hPa and above) tended to originate more from E-SE, especially those above the 700 hPa level. Since there is 1000 km of undisturbed rain forest in the NE direction seen from Balbina, and 200 km of forest to the SE, the Balbina site sampled in undisturbed air masses during the measurement campaign. *Kesselmeier et al.* [2000] measured very low values of benzene and toluene, that are otherwise tracers for anthropogenic influence. Ozone values were low and always <20 ppb.

[9] The particle measurements presented here were operated in near-continuous mode. It is therefore not surprising that intermittent observations of elevated particle concentrations (>1000 cm^{-3}) were made, indicating sources of local anthropogenic pollution such as transport of equipment to the site and maintenance work. These occurrences were removed from the data.

2.2. Instrumentation

[10] The sample flow was drawn from about 6 m above the ground into the field laboratory via an inlet system that was extended about 2 m above the roof of the laboratory, and had an aerodynamic cut-off diameter of 5 μm at ambient conditions.

[11] The Differential Mobility Particle Sizer (DMPS) was used to measure number-size distribution of aerosol particles with diameters in the range $3-850$ nm. The sheath flow was treated with diffusion dryers, and thus the particle size was measured in the dry condition (RH < 15%). Two Vienna-type DMAs [*Winklmayr et al.*, 1991] were used in parallel and covered particle sizes from 22 nm up to 850 nm and down to 3 nm respectively. Two condensation particle counters (CPC TSI 7610 and TSI 3025) were used for particle detection after each DMA. Both CPCs were calibrated for counting efficiency as a function of particle size. During the measurements, the two DMAs were operated in a stepwise scanning mode starting from 22 nm diameter and stepped upwards or downward respectively. Equal logarithmic diameter steps were used in the scans for a total of 36 mobility channels. A single scan over the whole size range took 15 min.

[12] The hygroscopic properties of aerosol particles were measured with a Hygroscopic Tandem Differential Mobility Analyzer (H-TDMA). The H-TDMA determines, in situ, the hygroscopic diameter growth of individual aerosol particles when taken from a dry state (RH < 5%) to a controlled humidified state. The H-TDMA consists mainly of three parts: (1) a DMA which selects a narrow, quasimonodisperse size range of the atmospheric aerosol at low RH; (2) humidifiers which condition the air to a well defined RH and (3) a second DMA which determines the change in diameter caused by the humidification. During the CLAIRE-98 experiment, the H-TDMA measurements were performed at 90% RH for six particle dry sizes (35, 50, 73, 109, 166 and 264 nm).

2.3. Data Inversion and Fitting

[13] The aerosol group in Lund has developed the inversion algorithms for both the DMPS and TDMA data [*Zhou*, 2001]. These programs are written in the LabVIEW graphical programming language [*National Instruments Corporation*, 1998], since the DMPS and TDMA data acquisition systems are operated in the LABVIEW interface.

[14] By taking into account the sampling line losses [*Hinds*, 1982], bipolar charging probabilities [*Wiedensohler*, 1988], calibrated DMA transfer functions regarding DMA diffusion broadening and losses [*Birmili et al.*, 1997], CPC counting efficiencies [*Wiedensohlet et al.*, 1997], the DMPS inversion program calculates the theoretical DMPS kernel transfer matrix and inverts mobility concentrations to an aerosol size distribution. In order to parameterize the inverted data, the aerosol size distributions were fitted to bimodal or trimodal lognormal distribution functions by minimizing the weighted-residual sum of squares according to the principles described in the CURFIT routine in the work of *Bevington* [1969]. The individual particle concentration values resulting from the inversion (dN/dlogDp) were used as weights during fitting. The fitting algorithm produces three parameters for each fitted mode: 1) the integral number, 2) the geometric mean diameter and 3) the geometric standard deviation of the mode.

[15] The TDMA fitting is based on the principles of TDMAFIT program [*Stolzenburg and McMurry*, 1988]. The primary parameters measured by the H-TDMA, and estimated by the data inversion routine for each particle group and dry size, are: 1) arithmetic mean diameter growth factor, 2) diameter growth dispersion factor and 3) relative number of particles (number fraction) in each hygroscopic particle group.

2.4. Internal Consistency Tests of the DMPS Data

[16] Two tests of the internal consistency for the DMPS measurements were made. The particle total number concentrations were integrated from DMPS measuring channels, and were compared with particle concentrations counted by a CPC (TSI 3010) through the entire campaign and when both the CPC and the DMPS were working properly. The comparison showed very good agreement and the differences were within an acceptable error limit. The R-squared value for the regression statistics was 0.91 and the integrated DMPS concentration was slightly higher than the CPC measured total aerosol concentration. The discrepancy is likely due to: 1) Particles smaller than 15 nm had about 5% (median value) of the total particle number concentrations, but were only partly counted by the CPC3010; 2) Different sampling inlets were used for the DMPS and CPC3010; 3) The low sampling flow of the CPC3010 (1 l/min) produced inlet losses that could not be corrected.

[17] Another test of the consistency of the concentration measurements is the comparison of mass concentration between the DMPS and rotating microorifice uniform deposit cascade impactor (MOUDI) [*Roberts et al.*, 2002]. The MOUDI impactor collected particles at ambient RH with 50% cut-off aerodynamic diameters of 0.093, 0.175, 0.33, 0.56 µm in the submicrometer size range. The cut-off sizes of the impactor stages are defined in equivalent aerodynamic diameters (EAD), while the DMA measures electrical mobility diameter (Stokes diameter) [*Hinds*, 1982]. The aerodynamic diameters were therefore converted to the corresponding Stokes diameters assuming that the particles were spherical and had a density of 1.15 g/cm^3 at ambient RH [*Swietlicki et al.*, 1999]. Since the DMPS measured the dry aerosol size distribution, ambient RH and H-TDMA hygroscopic growth data were used to convert the distribution to that ambient RH. The comparison was made for 7 MOUDI samples covering all concurrent MOUDI-DMPS measurements. Under an assumption of a dry particle density of 1.5 g/cm^3 [*Roberts et al.*, 2002], DMPS measurements agreed well with the MOUDI data for 0.093–0.56 µm EAD particles, with mass discrepancies of less than 30%.

## 2.5. Quality Assurance and Growth Factor Correction of TDMA Data

[18] Accurate measurement, control and monitoring of temperature, humidity and flow in the TDMA are needed for the determination of hygroscopic growth. The vital quality assurance parameters were logged continuously and had to satisfy certain requirements in order for the data to be accepted. The criteria are similar to those applied to the H-TDMA data during the ACE-2 experiment [*Swietlicki et al.*, 2000] regarding the stabilities in flows, pressures, RHs and particle counting. The error in measured growth factor is estimated to be ±0.05 relative units. This is a result of humidity fluctuations and humidity gradients in the second DMA and errors in modal values from counting and curve fitting uncertainty. The function of the equipment was regularly checked for growth at the nominal RH with standard aerosol of pure ammonium sulphate or sodium chloride. The growth factors of the test aerosols agreed with modelled growth [*Tang and Munkelwitz*, 1994; *Tang*, 1997] within the error estimated above.

[19] Although all possible efforts were made to ensure stable RH, postexperiment evaluation of instrument performances showed that the actual measurement RH deviated slightly from the nominal values (90 ± 3% RH). The measured growth factors needed to be corrected from the measurement RH to the nominal values. Previous aerosol measurements in the Amazon Basin during the wet season show that sulphate is the dominating ion for fine aerosols and the molar ratio of ammonium/sulphate is near to 1:1 [*Gerab et al.*, 1998]. The corrections of hygroscopic growth factors were therefore made by assuming that the particle soluble fraction only consisted of ammonium hydrogen sulphate [*Swietlicki et al.*, 2000]. Since the actual RH during the measurement was close to the nominal RH, the correction is rather small and depends only slightly on the assumption of ionic compound.

3. Results and Discussion

### 3.1. Aerosol Particle Concentration and Size Distribution

[20] The particle size distributions of atmospheric submicron aerosols (3–850 nm) were measured continuously between 27 March 1998 and 14 April 1998. The observed total number concentrations in the Amazon rain forest during the wet season are plotted in Figure 1, with the rain events on the same timescale. Several short incidents of elevated particle concentrations (>1000 cm^{-3}) were most likely caused by local anthropogenic pollution sources, and
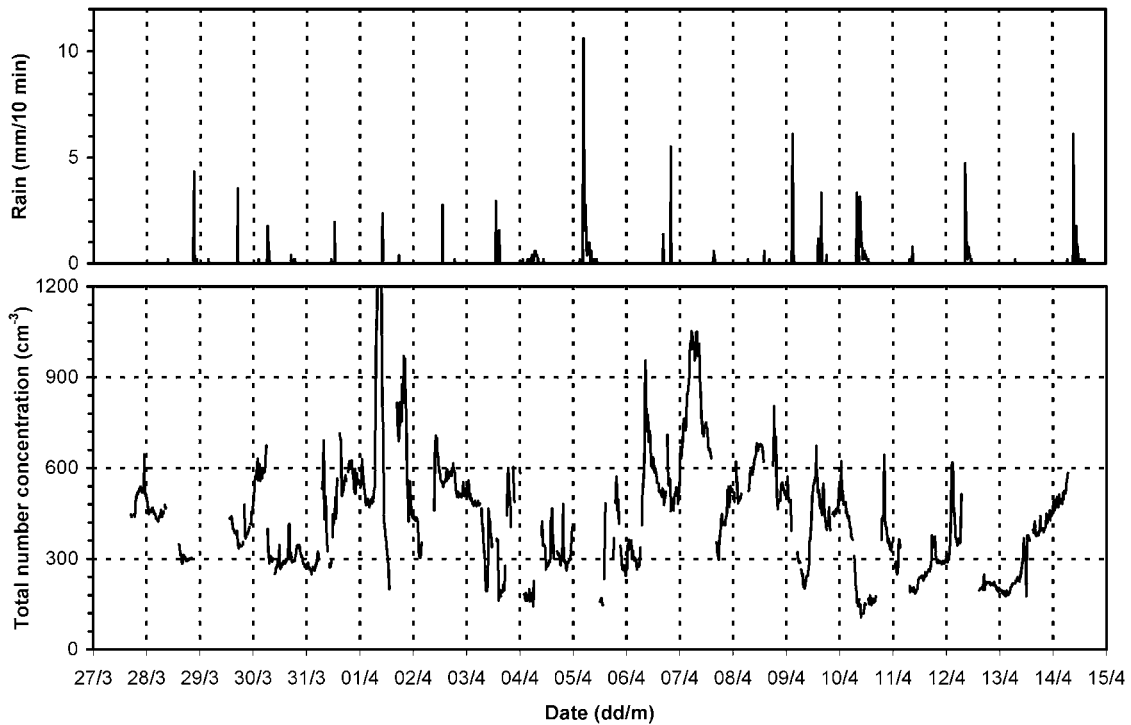
Figure 1. Particle total number concentrations during the CLAIRE-98 experiment. Local pollution events were removed. The rain events are also shown in the same time series.

were removed from the data. High particle concentrations that showed a more systematic temporal behavior were however included. In total, 5% of the data were removed. Low particle concentrations were normally observed after raining, as a result of wet deposition. For most of the measurement time during the experiment, the total particle concentrations were around 450 cm^{-3}, representative of a background Amazonian aerosol.
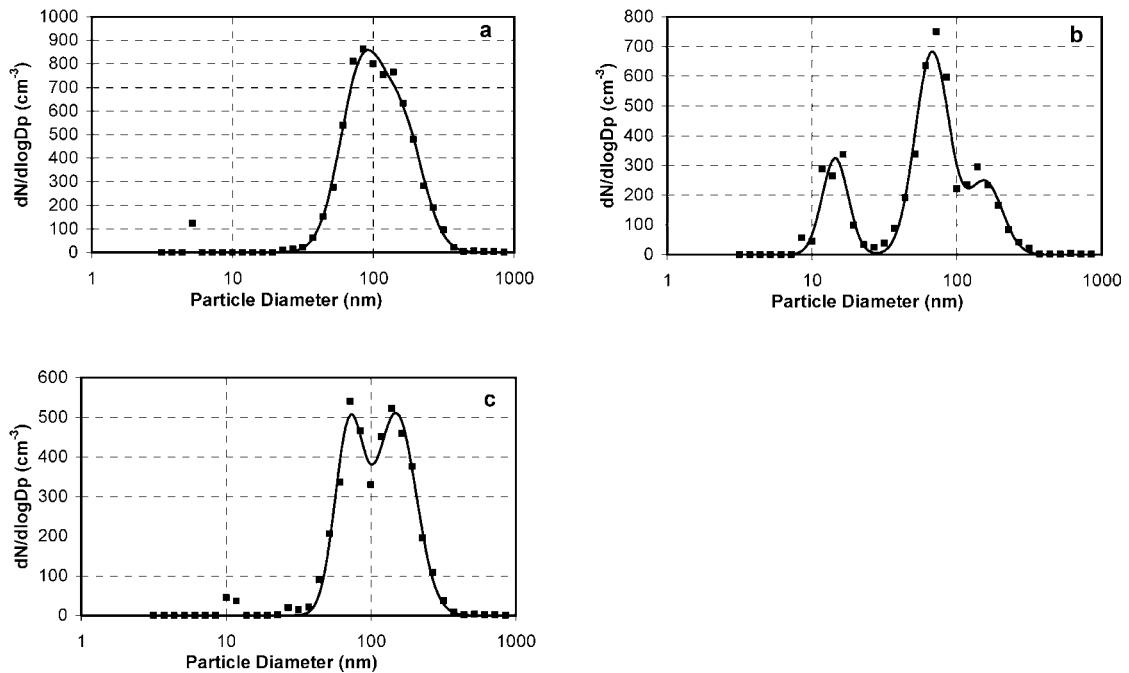
Figure 2. Particle number size distributions dN/dlogDp; examples of the measured data and lognormal fits on 30 March 1998. Squares are measured data; solid lines are the fitted log normal modes. (a) 0000 local standard time (LST), Aitken and accumulation modes are minimally separated. (b) 1145 LST, three separated modes were present. (c) 1500 LST, typical bimodal distribution.
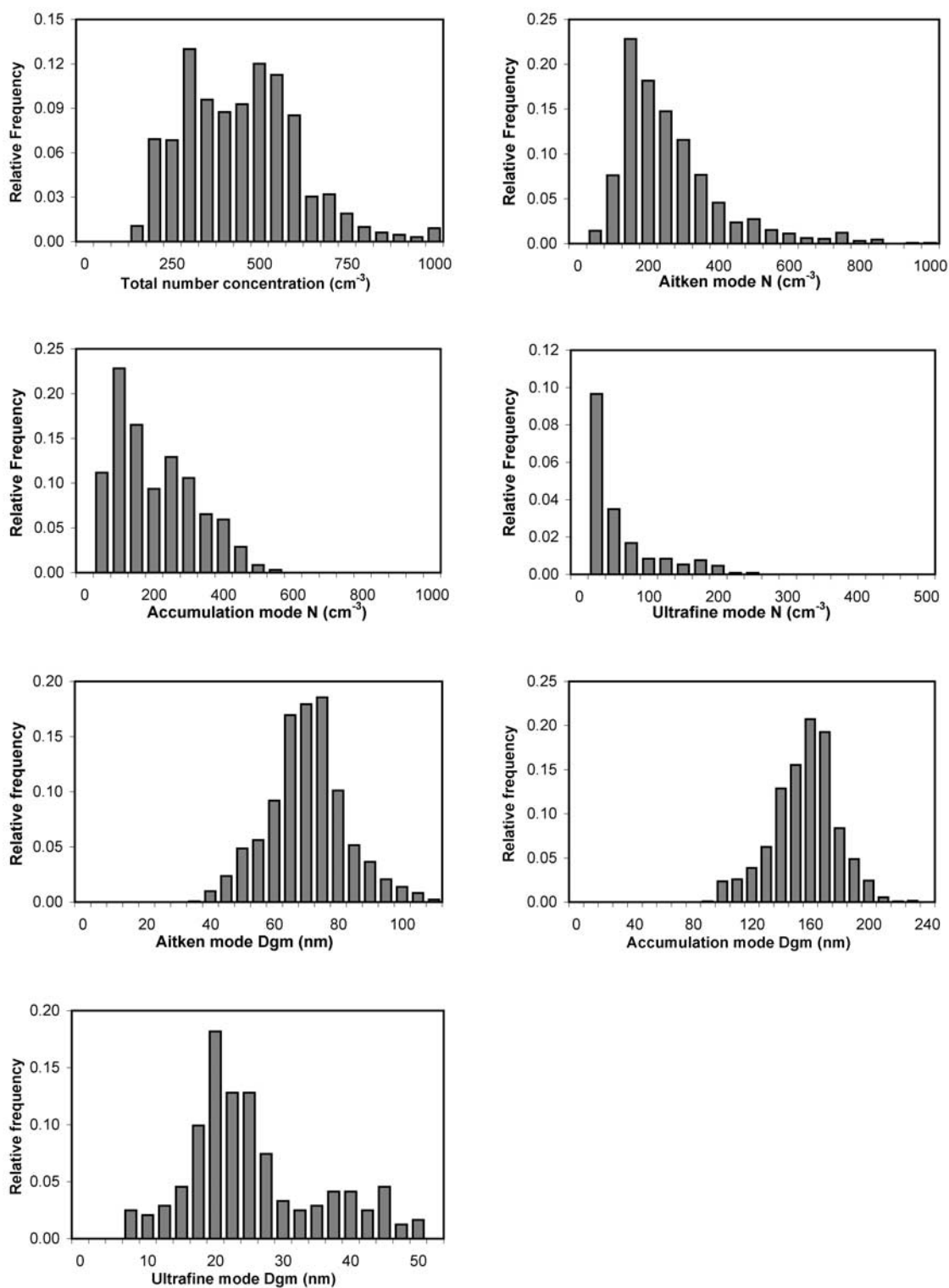
Figure 3. Histograms of the relative frequency of occurrence of the modal concentration (N) and geometric mean diameter (Dgm) for the fitted size distribution.

[21] Three selected number-size distributions were plotted in Figure 2 as examples of the DMPS measurements data and their lognormal fits. Three aerosol number-size distributions were taken from 30 March 1998. In Figures 2a and 2c, the particle size distributions are bimodal (Aitken and accumulation modes). These two modes were observed in all cases during the experiment. When a third mode appeared at smaller sizes (see example in Figure 2b), this was denoted the ultrafine mode. Note that this definition sometimes causes the geometric mean diameter of the ultrafine mode to reach as high as 50 nm (Figure 3). The ultrafine particle mode only occurred temporarily.

Table 1. Statistics of Particle Number Size Distribution During the CLAIRE-98 Experiment[a]

Mode	Frequency of Occurrence, %	Number Concentration, #/cm³			Geometric Mean Diameter, nm	Geometric Standard Deviation
		Mean ± Standard Deviation	Geometric Mean	Median		
Aitken	100	239 ± 154	200	200	68 ± 12	1.40 ± 0.14
Accumulation	100	177 ± 115	137	146	151 ± 22	1.40 ± 0.10
Ultrafine	18	92 ± 99	55	48	24 ± 10	1.31 ± 0.15

[a] A total of 1315 fifteen-minute spectra were fitted with two or three lognormal distributions.

The statistics of all parameters for the fitted modes are given in Table 1.

3.2. Frequency of Occurrence Statistics

[22] Histograms of the relative frequency of occurrence of the modal parameters of concentration and geometric mean diameter for the fitted size distribution are shown in Figure 3. The histograms of the number concentration data were not normally distributed but skewed with a tail toward high values. That indicates that mean values were not necessarily the most appropriate measures of central tendency of the distributions. Therefore, geometric means, median values were also calculated and given in Table 1 for comparison.

[23] There are several features that can be derived from the statistical analysis. The first is that the particle concentrations for the modes varied substantially, while the mean diameters did not. Another feature is the low concentrations of the ultrafine particle mode; the median concentration of ultrafine particles was only about 24% and 33% compared to the Aitken and accumulation mode particles respectively. Furthermore, while no correlation have been found between

diameter and concentration for ultrafine and Aitken mode particles, the correlation coefficient is negative (−0.66) for accumulation mode particles. This may be an indication that aged accumulation mode aerosols are associated with lower number concentrations and higher mean diameters.

3.3. Processes Controlling the Amazonian Aerosol Evolution

[24] The time series of the mean diameters for the three modes are presented in Figure 4. Both the Aitken and accumulation modes were continuously present, while the ultrafine mode was observed only temporarily. Their occurrence could in most cases be linked to incidences of local pollution, as for instance those coinciding or appearing close in time with the events of particle concentrations >1000 cm⁻³ on 3, 5, 8, 9, 10, and 12 April (removed from the data). In general, particles in the Aitken mode were observed at their lowest sizes (down to ∼30 nm) shortly after sunrise (0600 local time). In the absence of early morning rain, the Aitken mode particles concentrations also rose simultaneously (31 March, 1 and 6 April), indicating a
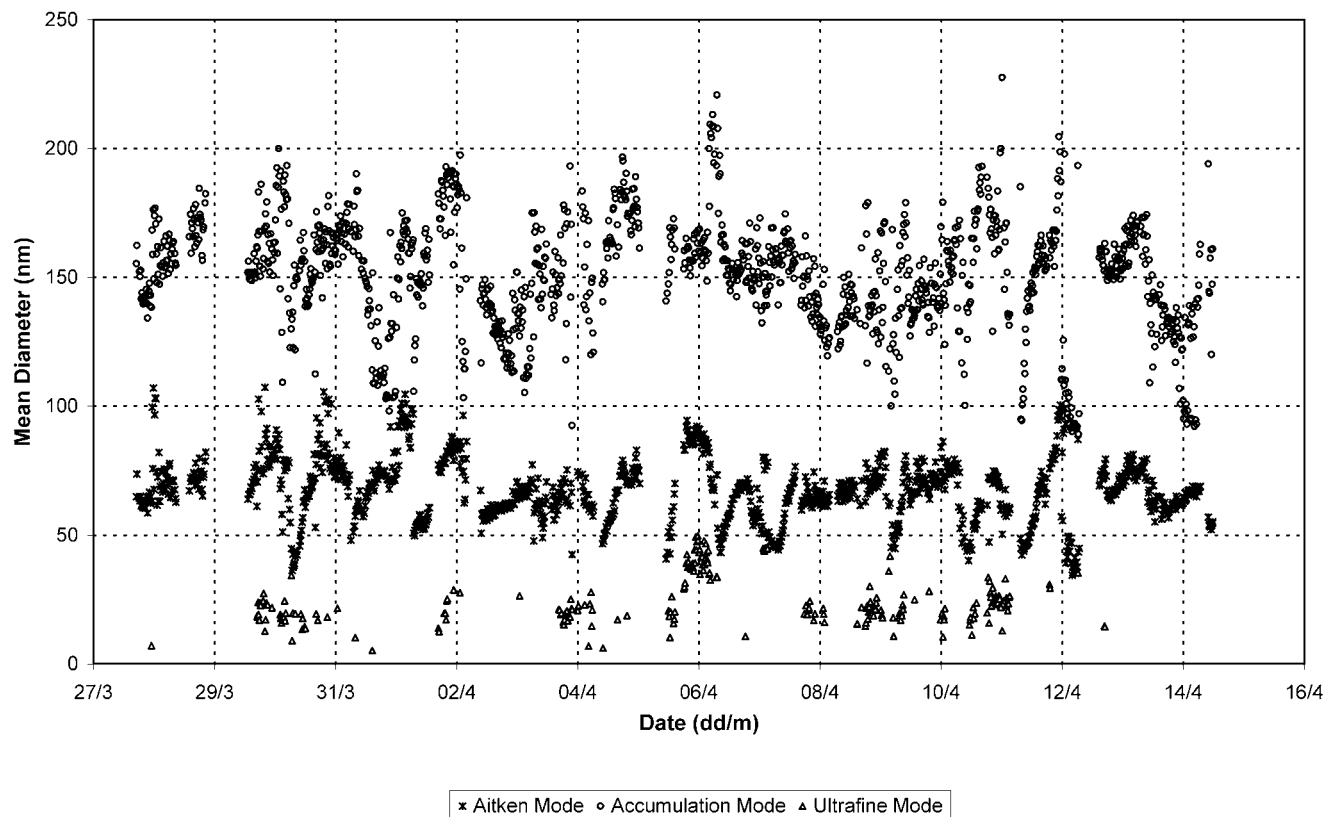
Figure 4. Time series of the geometric mean diameters of the aerosol particles during the CLAIRE-98 experiment.

Table 2. Summary of the H-TDMA Observations of Aerosol Hygroscopic Properties Made at Balbina Site During the CLAIRE-98 Experiment

Growth Factor at 90% RH	Dry Particle Diameter (nm)					
	35	50	73	109	166	264
Total number of observations	192	247	252	251	248	231
Less Hygroscopic Particles						
Growth factor (average ± 1 standard deviation)	1.17 ± 0.05	1.16 ± 0.04	1.17 ± 0.04	1.22 ± 0.06	1.26 ± 0.07	1.32 ± 0.07
Soluble fraction (average ± 1 standard deviation)	0.17 ± 0.05	0.15 ± 0.04	0.14 ± 0.04	0.18 ± 0.06	0.21 ± 0.07	0.27 ± 0.08
Number fraction (when present)	0.96 ± 0.13	0.97 ± 0.10	0.96 ± 0.14	0.93 ± 0.19	0.94 ± 0.15	0.97 ± 0.10
Frequency of occurrence (%)	100	95	94	96	95	97
Hydrophobic Particles						
Growth factor (average ± 1 standard deviation)	1.05 ± 0.03	1.05 ± 0.03	1.03 ± 0.03	1.02 ± 0.03	1.01 ± 0.03	1.03 ± 0.03
Soluble fraction (average ± 1 standard deviation)	0.05 ± 0.03	0.04 ± 0.03	0.03 ± 0.02	0.02 ± 0.02	0.01 ± 0.02	0.02 ± 0.02
Number fraction (when present)	0.32 ± 0.19	0.38 ± 0.18	0.45 ± 0.20	0.46 ± 0.25	0.31 ± 0.19	0.24 ± 0.17
Frequency of occurrence (%)	6	5	9	13	14	11
More Hygroscopic Particles						
Growth factor (average ± 1 standard deviation)	1.49 ± 0.10	1.38 ± 0.14	1.38 ± 0.10	1.42 ± 0.05	1.45 ± 0.05	1.54 ± 0.05
Soluble fraction (average ± 1 standard deviation)	0.60 ± 0.16	0.41 ± 0.19	0.37 ± 0.12	0.40 ± 0.07	0.42 ± 0.06	0.52 ± 0.07
Number fraction (when present)	0.37 ± 0.11	0.68 ± 0.40	0.85 ± 0.30	0.83 ± 0.31	0.82 ± 0.27	0.96 ± 0.11
Frequency of occurrence (%)	7	9	6	6	7	3

The results are expressed as average hygroscopic growth factors — defined as the particle diameter at the nominal RH = 90% divided by the diameter at RH < 10% — for the various mixed particle groups showing different hygroscopic properties. The average soluble fractions were calculated under the assumption that only ammonium hydrogen sulphate contributed to the hygroscopic growth. The number fraction is the relative number of particles in each hygroscopic particle group. The frequency of occurrence refers to the relative number of fitted observations.

new source of particles. The particles then grew in size during the course of the day at diameter growth rates of ~5 nm · h^{-1} (Figure 4). When new particles are formed by homogeneous nucleation of gas phase precursors, the critical cluster size is ~1 nm [*Kulmala et al.*, 2000]. Since no particles appeared systematically at the lowest size of detection (3 nm) outside the local pollution events, it can be concluded that the particles in the ultrafine and lower Aitken mode size ranges were not formed directly at the place of observation close to the ground by homogeneous nucleation, at least not in large numbers. For comparison, clear cases of particle growth starting at 3 nm was seen in a boreal forest [*Kulmala et al.*, 2000].

[25] Studies of the Amazonian boundary layer [*Martin et al.*, 1988] (G. Fisch et al., The convective boundary layer over pasture and forest in Amazonia, submitted to *Journal of Geophysical Research*, 2001, hereinafter referred to as G. Fisch et al., submitted manuscript, 2001) have identified a typical diurnal variation. A shallow (~100 m) nocturnal stable layer capped by a strong inversion is formed overnight. At sunrise, this layer starts breaking up as the ground heats. This causes gradual entrainment of air from the overlying residual layer — the remnant of the mixed boundary layer of the previous day. In the rain forest during the wet season, the mixed layer height was seen to increase rapidly (~100 m · h^{-1}) between 8:00 and 14:00 local time and reach a maximum height of ~1000 m shortly before sunset [G. Fisch et al., submitted manuscript, 2001]. Gases and particles in the residual layer are thus efficiently mixed down to ground level during daytime. At the same time, ground-level air constituents are also dispersed to higher altitudes. No systematic decreases in accumulation mode particle concentrations were observed after sunrise that might have indicated the dispersal of these particles from a ground-level source into a larger volume. Shallow (3–4 km) and deep convection (~10 km) are other mechanisms for efficient — although more intermittent — air mass exchange between the well-mixed

boundary layer and the overlying troposphere [*Andreae et al.*, 2001]. The intense daytime radiation also triggers gas phase photochemical reactions involving hydroxyl radicals and ozone as oxidants, converting precursor gaseous species into less volatile oxygenated compounds.

[26] The main volatile organic components in the gas phase were isoprene and formaldehyde, while various monoterpenes were found at considerable smaller concentrations — total monoterpene concentrations were below 1 ppb [*Kesselmeier et al.*, 2000]. Isoprene and formaldehyde do not produce secondary organic aerosol mass through photochemical reactions, and are therefore not likely candidates as precursors of secondary aerosol mass [*Seinfeld and Pandis*, 1998]. Furthermore, the low concentrations of isoprene oxidation products and ozone daily maximum <20 ppb led *Kesselmeier et al.* [2000] to conclude that the oxidation capacity of the lower atmospheric boundary layer during CLAIRE-98 was low.

[27] Nevertheless, a large portion of the aerosol mass during CLAIRE-98 consisted of secondary organic compounds [*Kubátová et al.*, 2000]. Dicarboxylic acids and related oxidative degradation products were identified and were confined mostly to the fine fraction aerosol. Although no firm conclusions could be drawn, *Kubátová et al.* [2000] suggested that the organic compounds they observed were oxidation products of biogenic monoterpenes and fatty acids. Furthermore, the low hygroscopic growth of the Aitken mode particles (Table 2) resembled that observed in photo-reactor studies of monoterpene oxidation products [*Virkkula et al.*, 1999].

[28] The available data set precludes a firm statement to be made regarding the origin of the observed ultrafine and Aitken mode particles, but it is unlikely that they were formed at ground level by homogeneous nucleation of gas phase precursors. Instead, the most probable source is mixing from aloft. The particle formation mechanism remains uncertain, but ternary nucleation of NH_3-H_2SO_4-H_2O is one
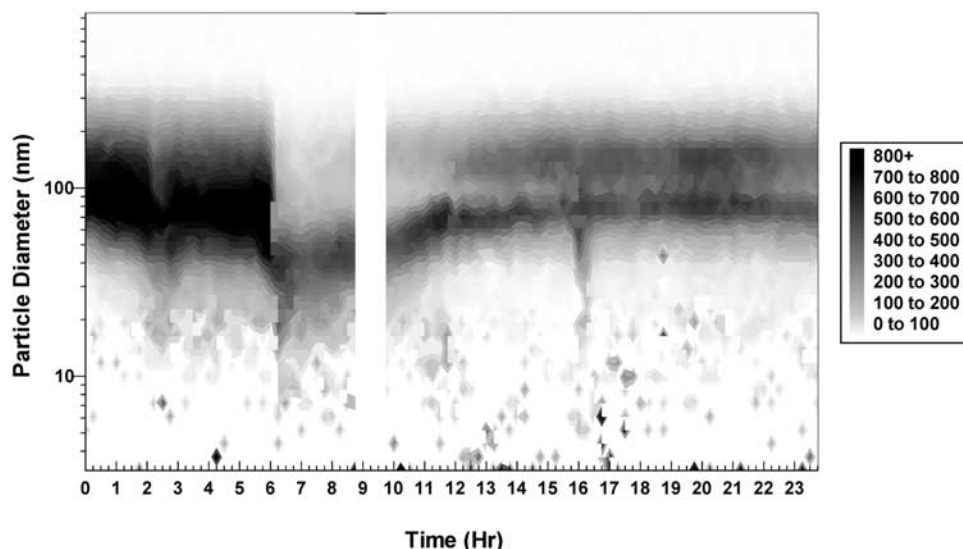
Figure 5. Three dimension contour plot of the aerosol number-size distribution on 30 March 1998. Major rain events were at 0600 and 1650 (see Figure 2).

possible candidate [*Kulmala et al.*, 2000]. The location of formation—in the residual layer, the entrainment region, or above—is also unclear. The observed growth at ∼5 nm · h^{-1} is most likely caused by condensation of low-volatility vapours of biogenic origin. The accumulation mode particles are believed to have formed via in-cloud processing of Aitken mode particles, leading to fixation of soluble gases (e.g., SO$_2$) in the evaporating droplets. It is obvious that wet deposition is a vital removal mechanism for particles in the both the accumulation and Aitken mode size ranges. Figure 5 shows an example of a time sequence including extensive wet deposition during an early morning rain, the appearance of a new Aitken mode and its subsequent growth to larger sizes, and finally the appearance of an accumulation mode as a result of cloud processing.

3.4. Hygroscopic Growth

[29] The H-TDMA measurements were made more or less continuously during the experiment except for some power failure events. The growth factors were measured at 90% RH for six particle sizes: particles with diameters at 35, 50 and 73 nm are Aitken mode particles, while those at 109, 166 and 264 nm are accumulation mode particles.

[30] Even though three hygroscopic particle types were observed during the experiment, most observations showed a unimodal hygroscopic behavior with only the low-growth group present, denoted less hygroscopic particles. The remaining two hygroscopic groups are denoted hydrophobic and more hygroscopic. The less hygroscopic particles essentially represent the aerosol in the pristine Amazon forest. The diameter growths of the less hygroscopic particles were different for Aitken and accumulation particles. While the diameter growth factors of Aitken particles were nearly constant over particle dry sizes, the diameter growth factors of accumulation particles increased with particle dry sizes. This indicates that the accumulation mode particles were formed via in-cloud processing of activated Aitken mode particles through fixation of SO$_2$. The hydrophobic and more hygroscopic particles can only be observed in a few percent of the cases. The hydrophobic particles were defined when

their diameter growth factor was less than 1.1 and the less hygroscopic group was also present. The occurrence of hydrophobic particles is likely a sign of recent anthropogenic influence [*Weingartner, et al.*, 1995, 1997]. The more hygroscopic group was mainly observed in the beginning of the experiment, when Earth probe TOMS and filter-impactor analysis suggested that the station was influenced by an outbreak of Saharan dust and biomass burning [*Maenhaut et al.*, 1998; *NASA*, 1998, available at http://toms.gsfc.nasa.gov/aerosols/aerosols.html; *Rajta et al.*, 1998]. Occasionally, both more hygroscopic particles and less hygroscopic particles were found. Table 2 summarized the TDMA data observed during the course of the experiment.

[31] Under the assumption that only ammonium hydrogen sulphate contributed to the hygroscopic growth, the average soluble volume fractions for all particle dry sizes and hygroscopic groups were calculated and given in Table 2. Combined with the DMPS size distribution data, the average soluble volume fraction of submicrometer aerosol particles was calculated to be about 23%. This result showed a good agreement with the concurrent stack filter unit measurement [*Maenhaut et al.*, 1998], where the inorganic aerosols were accounting for 22% of the total mass in the fine mode aerosol (aerodynamic cut-off diameter = 2 μm).

3.5. Comparison of Measured and Modelled CCN Concentrations

[32] Concentrations of cloud condensation nuclei (CCN) at six supersaturations from 0.15% to 1.5% were measured during the CLAIRE-98 experiment [*Roberts et al.*, 2002]. The CCN concentration can also be modelled via Köhler theory from the aerosol particle number-size distribution and additional information about the chemistry or hygroscopic properties of the aerosol particles [*Covert et al.*, 1998].

[33] A detailed discussion on CCN properties can be found in the work of [*Roberts et al.*, 2002]. Here, hygroscopic growth data were used to estimate the aerosol particle composition and solubility with a much higher time resolution than would be possible from impactor chemical data alone. The particles were assumed to be composed

Table 3. Comparison of Measured and Modelled CCN Concentrations During the CLAIRE-98 Experiment[a]

S, %	0.15	0.30	0.60	1.00	1.50
MR(o/p)	0.43	0.67	0.70	0.76	0.83
N	1488	1531	1257	1228	968
R	0.68	0.81	0.84	0.83	0.87

[a] S is the supersaturation of the CCN measurement. MR(o/p) represents the median ratio of observed to predicted CCN concentration; N is the number of comparing observations and R is the correlation coefficient.

ammonium hydrogen sulphate and an insoluble volume fraction. Köhler theory [*Pruppacher and Klett*, 1997, pp. 172–178] was then applied to determine the minimum particle diameter (the critical diameter) that would activate at the supersaturations prevailing in the CCN counter during the actual measurements. The aerosol number-size distributions were integrated for diameters greater than the critical values and compared to the measured CCN concentrations.

[34] The CCN concentrations are estimated for the concurrent CCN-DMPS-TDMA observations through the experiment (Table 3). The reasons for overprediction of CCN concentrations compared to the actual CCN measurements are not clear. Similar results were obtained at Cape Grim, Tasmania during the ACE-1 experiment [*Covert et al.*, 1998] (~20% overprediction at 0.5% supersaturation) and in the Arctic Ocean during the AOE96 experiment [*Zhou et al.*, 2002] (~30% overprediction at around 0.25% supersaturation).

4. Conclusions

[35] The number-size distribution and hygroscopic growth of the submicrometer aerosol particles were measured in the Amazon rain forest during the first LBA-CLAIRE experiment in March–April 1998. This was the first time ever that these types of measurement were performed in the Amazon rain forest.

[36] The observed total aerosol particle number concentration in the size range 3–850 nm was around 450 cm^{-3}. Since Aitken and accumulation mode particles were ubiquitous, the typical wet season submicrometer aerosol can be represented by a bimodal number-size distribution. An ultrafine mode only occurred in 18% of the cases, resulting in a trimodal distribution. However, the appearance of the ultrafine particles was not systematic and could in nearly all cases be linked to local anthropogenic pollution. This leads to the conclusion that new ultrafine particles were not formed at ground level by homogeneous nucleation of gas phase precursors. The occurrence of particles in the lower Aitken mode size range (down to 30 nm) coincided with the break-up of the nocturnal boundary layer and mixing with the overlying air. During daytime, Aitken mode diameter growth rates of ~5 nm · h^{-1} were observed, causing the geometric mean diameter of this mode to increase from about 35 to 80 nm. This growth was probably due to condensation of low-volatility vapours of biogenic origin. There were no indications of a ground-level natural source of accumulation mode particles. Instead, these particles are believed to be have been formed by cloud processing of Aitken mode particles. Wet deposition is an important removal mechanism for particles in both the accumulation and Aitken mode size ranges.

[37] The hygroscopic properties of aerosol particles (35–265 nm) in the Amazon rain forest are essentially unimodal with diameter growth factors (from dry to 90% RH) between 1.16–1.32. This growth is low compared to those found in other types of aged aerosols, for instance in remote marine environments. The reason is that the submicrometer aerosol particles in Amazonia contain only a small fraction of soluble inorganic compounds. Instead, organic species with low affinity for water dominate the fine fraction aerosol.

[38] Predictions of CCN concentrations based on particle number-size distributions and hygroscopic properties partly overestimated the actual measured CCN concentrations. The discrepancy was similar to that found in other remote environments. This means that the wet season CCN activity can be fairly well estimated by use of a simple model that need not include a detailed description of the composition and hygroscopic properties of the organic aerosol fraction.

References

Andreae, M. O., et al., Transport of biomass burning smoke to the upper troposphere by deep convection in the equatorial region, *Geophys. Res. Lett.*, *28*, 951–954, 2001.

Artaxo, P., H. Storms, F. Bruynseels, R. V. Grieken, and W. Maenhaut, Composition and sources of aerosols from the Amazon Basin, *J. Geophys. Res.*, *93*, 1605–1615, 1988.

Artaxo, P., W. Maenhaut, H. Storms, and R. V. Grieken, Aerosol characteristics and sources for the Amazon Basin during the wet season, *J. Geophys. Res.*, *95*, 16,971–16,985, 1990.

Artaxo, P., E. T. Fernandes, J. V. Martins, M. A. Yamasoe, P. V. Hobbs, W. Maenhaut, K. M. Longo, and A. Castanho, Large-scale aerosol source apportionment in Amazonia, *J. Geophys. Res.*, *103*, 31,837–31,847, 1998.

Bates, T. S., V. N. Kapustin, P. K. Quinn, D. S. Covert, D. J. Coffman, C. Mari, P. A. Durkee, W. J. DeBruyn, and E. S. Saltzman, Processes controlling the distribution of aerosol particles in the lower marine boundary layer during the First Aerosol Characterization Experiment (ACE 1), *J. Geophys. Res.*, *103*, 16,369–16,383, 1998.

Berg, O. H., E. Swietlicki, and R. Krejci, Hygroscopic growth of aerosol particles in the marine boundary layer over the Pacific and Southern Oceans during ACE-1, *J. Geophys. Res.*, *103*, 16,535–16,545, 1998.

Bevington, P. R., *Data Reduction and Error Analysis for the Physical Sciences*, McGraw-Hill, New York, 1969.

Birmili, W., F. Stratmann, A. Wiedensohler, D. Covert, L. M. Russell, and O. Berg, Determination of differential mobility analyzer transfer functions using identical instruments in series, *Aerosol Sci. Technol.*, *27*(2), 215–223, 1997.

Browell, E. V., G. L. Gregory, R. C. Harriss, and V. W. J. H. Kirchhoff, Tropospheric ozone and aerosol distribution across the Amazon Basin, *J. Geophys. Res.*, *93*, 1431–1451, 1988.

Browell, E. V., G. L. Gregory, R. C. Harriss, and V. W. J. H. Kirchhoff, Ozone and aerosol distributions over the Amazon Basin during the wet season, *J. Geophys. Res.*, *95*, 16,887–16,901, 1990.

Covert, D. S., V. N. Kapustin, T. S. Bates, and P. K. Quinn, Physical properties of the marine boundary layer aerosol particles of the mid-Pacific in relation to sources and meteorological transport, *J. Geophys. Res.*, *101*, 6919–6930, 1996a.

Covert, D. S., A. Wiedensohler, P. P. Aalto, J. Heintzenberg, P. H. McMurry, and C. Leck, Aerosol number size distributions from 3 to 500 nm diameter in the arctic marine boundary layer during summer and autumn, *Tellus*, *48B*, 197–212, 1996b.

Covert, D. S., J. L. Gras, A. Wiedensohler, and F. Stratmann, Comparison of directly measured CCN with CCN modelled from the number-size distribution in the marine boundary layer during ACE 1 at Cape Grim, Tasmania, *J. Geophys. Res.*, *103*, 16,597–16,608, 1998.

Echalar, F., P. Artaxo, J. V. Martins, M. Yamasoe, F. Gerab, W. Maenhaut, and B. Holben, Longterm monitoring of atmospheric aerosols in the Amazon Basin: Source identification and apportionment, *J. Geophys. Res.*, *103*, 31,849–31,864, 1998.

Eck, T. F., B. N. Holben, I. Slutsker, and A. Setzer, Measurements of irradiance attenuation and estimation of aerosol single scattering albedo for biomass burning aerosols in Amazonia, *J. Geophys. Res.*, *103*, 31,865–31,878, 1998.

Flagan, R. C., History of electrical aerosol measurements, *J. Aerosol Sci.*, *28*(4), 301–380, 1998.

Garstang, M., et al., Trace gas exchange and convective transports over the Amazonian rain forest, *J. Geophys. Res.*, *93*, 1528–1550, 1988.

Gerab, F., P. Artaxo, R. Gillet, and G. Ayers, PIXE, PIGE and ion chromatography of aerosol particles from northeast Amazon Basin, *Nucl. Instrum. Methods B*, *136–138*, 955–960, 1998.

Gregory, G. L., E. V. Browell, and L. S. Warren, Amazon Basin ozone and aerosol: Wet season observations, *J. Geophys. Res.*, *95*, 16,903–16,912, 1990.

Harriss, R. C., et al., The Amazon boundary layer experiment (ABLE 2A): Dry season 985, *J. Geophys. Res.*, *93*, 1351–1360, 1988.

Harriss, R. C., et al., The Amazon boundary layer experiment: Wet season 1987, *J. Geophys. Res.*, *95*, 16,721–16,736, 1990.

Hinds, W. A., *Aerosol Technology*, John Wiley, New York, 1982.

Kaufman, Y. J., et al., Smoke, Clouds, and Radiation Brazil (SCAR B) experiment, *J. Geophys. Res.*, *103*, 31,783–31,808, 1998.

Kesselmeier, J., et al., Atmospheric volatile organic components (VOC) at a remote tropical forest in central Amazonia, *Atmos. Environ.*, *34*, 4063–4072, 2000.

Kotchenruther, R. A., and P. V. Hobbs, Humidification factors of aerosols from biomass burning in Brazil, *J. Geophys. Res.*, *103*, 32,081–32,089, 1998.

Kubátová, A., R. Vermeylen, M. Claeys, J. Cafmeyer, W. Maenhaut, G. Roberts, and P. Artaxo, Carbonaceous aerosol characterization in the Amazon basin, Brazil: Novel dicarboxylic acids and related compounds, *Atmos. Environ.*, *34*, 5037–5051, 2000.

Kulmala, M., L. Pirjola, and J. M. Mäkelä, Stable sulphate clusters as a source of new atmospheric particles, *Nature*, *404*, 66–69, 2000.

Maenhaut, W., I. Rajta, and J. Cafmeyer, Aerosol chemistry at Balbina, Brazil, during LBA-CLAIRE-98, paper presented at the 1998 Fall AGU Meeting, San Francisco, Calif., 6–10 Dec. 1998.

Martin, C. L., D. Fitzgarrald, M. Garstang, A. P. Oliveira, S. Greco, and E. Browell, Structure and growth of the mixing layer over the Amazonian rain forest, *J. Geophys. Res.*, *93*, 1361–1375, 1988.

National Aeronautics and Space Administration, *Earth Probe TOMS Aerosol Index*, Washington, D.C., 1998.

National Instruments Corporation, *BridgeVIEW*™ and *LabVIEW*™ G Programming Reference Manual, 1998.

Pruppacher, H. R., and J. D. Klett, *Microphysics of Clouds and Precipitation*, 954 pp., Kluwer Acad., Norwell, Mass., 1997.

Rajta, I., W. Maenhaut, and J. Cafmeyer, Detailed mass size distribution of atmospheric trace elements at Balbina, Brazil, during LBA-CLAIRE-98, paper presented at the 1998 Fall AGU Meeting, San Francisco, 6–10 December 1998.

Remer, L. A., Y. J. Kaufman, B. N. Holben, A. M. Thompson, and D. McNamara, Biomass burning aerosol size distribution and modeled optical properties, *J. Geophys. Res.*, *103*, 31,879–31,891, 1998.

Roberts, G., P. Artaxo, J. Zhou, E. Swietlicki, and M. O. Andreae, Sensitivity of CCN spectra on chemical and physical properties of aerosol: A case study from the Amazon Basin, *J. Geophys. Res.*, *107*, 10.1029/2001JD000583, in press, 2002.

Seinfeld, J. H., and S. N. Pandis, *Atmoshperic Chemistry and Physics*, John Wiley, New York, 1998.

Stolzenburg, M. R., and P. H. McMurry, *TDMAFIT User's Manual*, PTL Publ. 653, Particle Technology Laboratory, Department of Mechanical Engineering, University of Minnesota, Minneapolis, Minn., 1988.

Svenningsson, B. H. C. Hansson, B. Martinsson, A. Wiedensohler, E. Swietlicki, S. I. Cederfelt, M. Wendisch, K. N. Bower, T. W. Choularton, and R. N. Colvile, Cloud droplet nucleation scavenging in relation to the size and hygroscopic behaviour of aerosol particles, *Atmos. Environ.*, *31*, 2463–2475, 1997.

Swietlicki, E., et al., A closure study of sub-micrometer aerosol particle hygroscopic behaviour, *Atmos. Res.*, *50*, 205–240, 1999.

Swietlicki, E., et al., Hygroscopic properties of aerosol particles in the north-eastern Atlantic during ACE-2, *Tellus*, *52B*, 201–227, 2000.

Talbot, R. W., M. O. Andreae, T. W. Andreae, and R. C. Harriss, Regional aerosol chemistry of the Amazon Basin during the dry season, *J. Geophys. Res.*, *93*, 1499–1508, 1988.

Talbot, R. W., M. O. Andreae, H. Berresheim, P. Artaxo, M. Garstang, R. C. Harriss, K. M. Beecher, and S. M. Li, Aerosol chemistry during the wet season in central Amazonia: The influence of long-range transport, *J. Geophys. Res.*, *95*, 16,955–16,969, 1990.

Tang, I. N., Thermodynamic and optical properties of mixed-salt aerosols of atmospheric importance, *J. Geophys. Res.*, *102*, 1883–1893, 1997.

Tang, I. N., and H. R. Munkelwitz, Water activities, densities, and refractive indices of aqueous sulfates and sodium nitrate droplets of atmospheric importance, *J. Geophys. Res.*, *99*, 18,801–18,808, 1994.

Virkkula, A., R. VanDingenen, F. Raes, and J. Hjorth, Hygroscopic properties of aerosol formed by oxidation of limonene, alpha-pinene, and beta-pinene, *J. Geophys. Res.*, *104*, 3569–3579, 1999.

Wiedensohler, A., An approximation of the bipolar charge-distribution for particles in the sub-micron size range, *J. Aerosol Sci.*, *19*(3), 387–389, 1988.

Wiedensohlet, A., et al., Intercomparison study of the size-dependent counting efficiency of 26 condensation particle counters, *Aerosol Sci. Technol.*, *27*(2), 224–242, 1997.

Weingartner, E., U. Baltensperger, and H. Burtscher, Growth and structural change of combustion aerosols at high relative humidity, *Environ. Sci. Technol.*, *29*(12), 2982–2986, 1995.

Weingartner, E., H. Burtscher, and U. Baltensperger, Hygroscopic properties of carbon and diesel soot particles, *Atmos. Environ.*, *31*(15), 2311–2327, 1997.

Winklmayr, W., G. P. Reischl, A. O. Lindner, and A. Berner, A new electromobility spectrometer for the measurement of aerosol size distributions in the size range from 1 to 1000 nm, *J. Aerosol Sci.*, *22*(3), 289–296, 1991.

Wouters, L., S. Hagedoren, I. Dierck, P. Artaxo, and R. V. Grieken, Laser microprobe mass analysis of Amazon Basin, *Atmos. Environ.*, *27A*, 661–668, 1993.

Zhang, X. Q., P. H. McMurry, S. V. Hering, and G. S. Casuccio, Mixing characteristics and water content of submicron aerosols measured in Los Angeles and at the Grand Canyon, *Atmos. Environ.*, *27A*(10), 1593–1607, 1993.

Zhou, J., Hygroscopic properties of atmospheric aerosol particles in various environments, Ph.D. thesis, 166 pp., ISBN 91-7874-120-3, LUTFD2/(TFKF-1025)/1-166/(2001), Lund University, Lund, Sweden, 2001.

Zhou, J., E. Swietlicki, O. H. Berg, P. P. Aalto, K. Hämeri, E. D. Douglas, and C. Leck, Hygroscopic properties of aerosol particles over the central Arctic Ocean during summer, *J. Geophys. Res.*, *106*(23), 10.1029/2001JD900426, 2002.

————————

J. Zhou and E. Swietlicki, Division of Nuclear Physics, Lund University, P.O. Box 118, S-22100 Lund, Sweden. (erik.swietlicki@pixe.lth.se; jingchuan.zhou@nuclear.lu.se)

H. C. Hansson, Department of Meteorology, Stockholm University, S-10691 Stockholm, Sweden. (hc@misu.su.se)

P. Artaxo, Department of Physics, University of São Paulo, Caixa Postal 66318, CEP 05315-970, São Paulo, Brazil. (artaxo@if.usp.br)